Electronic supplementary information (ESI) for

Direct evaluation of hole effective mass of SnS-SnSe solid solutions with ARPES measurement

Issei Suzuki[*,a], Zexin Lin[a], Sakiko Kawanishi[a], Kiyohisa Tanaka[b], Yoshitaro Nose[c], Takahisa Omata[a], Shin-ichiro Tanaka[d]

[a] Institute of Multidisciplinary Research for Advanced Materials, Tohoku University, Katahira 2-1-1, Aoba-ku, Sendai 980-8577, Japan

[b] UVSOR Synchrotron Facility, Institute for Molecular Science, Okazaki 444-8585, Japan.

[c] Department of Materials Science and Engineering, Kyoto University, Yoshida-Honmachi, Sakyo-ku, Kyoto, 606-8501, Japan

[d] SANKEN, The Institute of Scientific and Industrial Research, Osaka University, 8-1 Mihogaoka, Ibaraki, Osaka 567-0047, Japan

E-mail: issei.suzuki@tohoku.ac.jp

Section 1. Materials preparation

$SnS_{1-x}Se_x$ single crystals were obtained by physical vapor transport using a Bridgman furnace following the same procedure for the growth of Zn_3P_2 crystals [S1]. Sn-S-Se alloys with predetermined compositions were used for the evaporation sources [S2]. The evaporation source was sealed in an evacuated quartz ampule with a length of 200 mm and an inner diameter of 11 mm. Subsequently, the ampule was set in a vertical Bridgman furnace. The temperature of the source placed at the bottom of the ampoule was maintained at 800 ºC, and the crystal was grown by cooling the opposite side (the top of the ampoule) from 800 to 700 ºC at 0.3 ºC/hour.

Section 2. Cleanness of the sample surfaces

The cleanness of the sample surface is crucial for surface-sensitive photoelectron spectroscopy measurements. In this study, the SnS-SnSe solid solution single crystal was cleaved in vacuum (< 1×10^{-8} Pa) immediately before the ARPES measurement. In this case, two possible causes of contamination to the sample surface can arise.

(a) Contamination introduced into the sample during the sample preparation and transportation in the air. This contamination is already present inside the sample before the sample cleavage.

(b) Contamination due to the adsorption of residual gas in the vacuum chamber onto the sample surface during storage and measurement after the sample cleavage. Such contamination is proportional to the [pressure in the chamber] × [sticking coefficient].

This study confirmed that the ARPES measurement was not affected by contamination of (a) or (b) due to the following three reasons.

(1) The observed ARPES spectra all exhibited very clear dispersions, attributed to SnS-SnSe solid solutions. Therefore, the contamination of (a) minimally affected the results and did not need to be considered in this study.

(2) The SnS single crystal was cleaved at ~3×10^{-7} Pa, and the survey XPS spectrum was obtained by laboratory XPS, as shown in Figure S1. Note that this single crystal was grown using the flux method[S3], which is different from the growth method employed for the samples subjected to the ARPES measurement in this study. Complete absence of C 1s or O 1s peaks were found, even after ~30 min of storage in the chamber. The laboratory XPS results showed that the sticking coefficient of the cleavage plane of the SnS single crystal was sufficiently small that no contamination occurred during storage in the high vacuum environment for a reasonable time. In this study, the SnS-SnSe solid solutions used had a similar crystal structure and electronic structure to the SnS single crystal. Therefore, the sticking coefficient was also considered to be similar. The vacuum at which the cleavage and measurement were performed in this study was even much better, < 1×10^{-8} Pa, and the measurement time was approximately ~5 h. Thus, no oxygen or carbon was expected to be absorbed onto the sample surface during the experiment in this study.

(3) In addition, peak fitting with two Gaussian peak lines was performed to the Sn 3d, S 2p, and Se 3d core levels of the $\mathrm{SnS}_{1-x}\mathrm{Se}_x$ (x=0, 0.51, 1) measured in the same setup as ARPES measurements. The fit is adequate, as shown in Figure S2 and Table S1. This result indicates that no compounds in different chemical states are present than $\mathrm{SnS}_{1-x}\mathrm{Se}_x$, such as SnO, $\mathrm{SnO_2}$, $\mathrm{SnS_2}$, and $\mathrm{SnSe_2}$, supporting the cleanness of the sample surface.

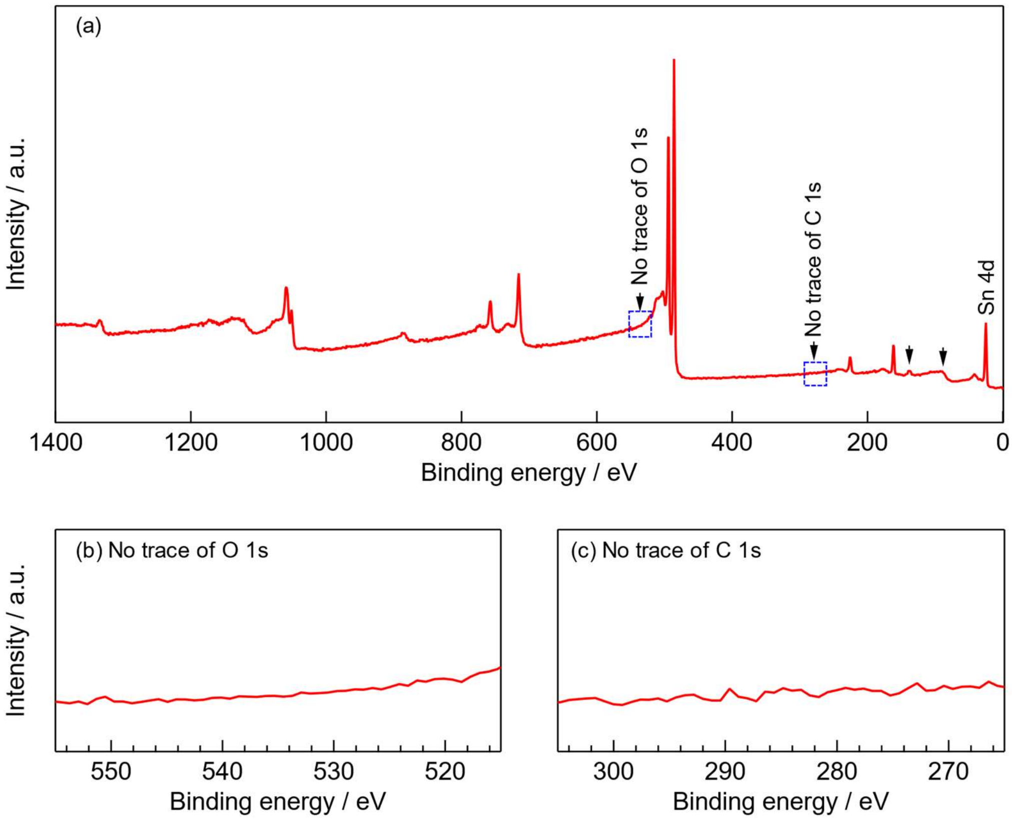

Figure S1. (a) Survey spectrum of the undoped SnS single crystal measured by the laboratory XPS. The measurement was performed after cleavage and following storage for ~30 min in vacuum at $\sim 3 \times 10^{-7}$ Pa. Complete absence of O 1s and C 1s peaks were found in the separated enlarged spectra in (b) and (c). Note that this single crystal was grown by the flux method [S3], which is different from a method employed to the sample in this study for the ARPES measurements.

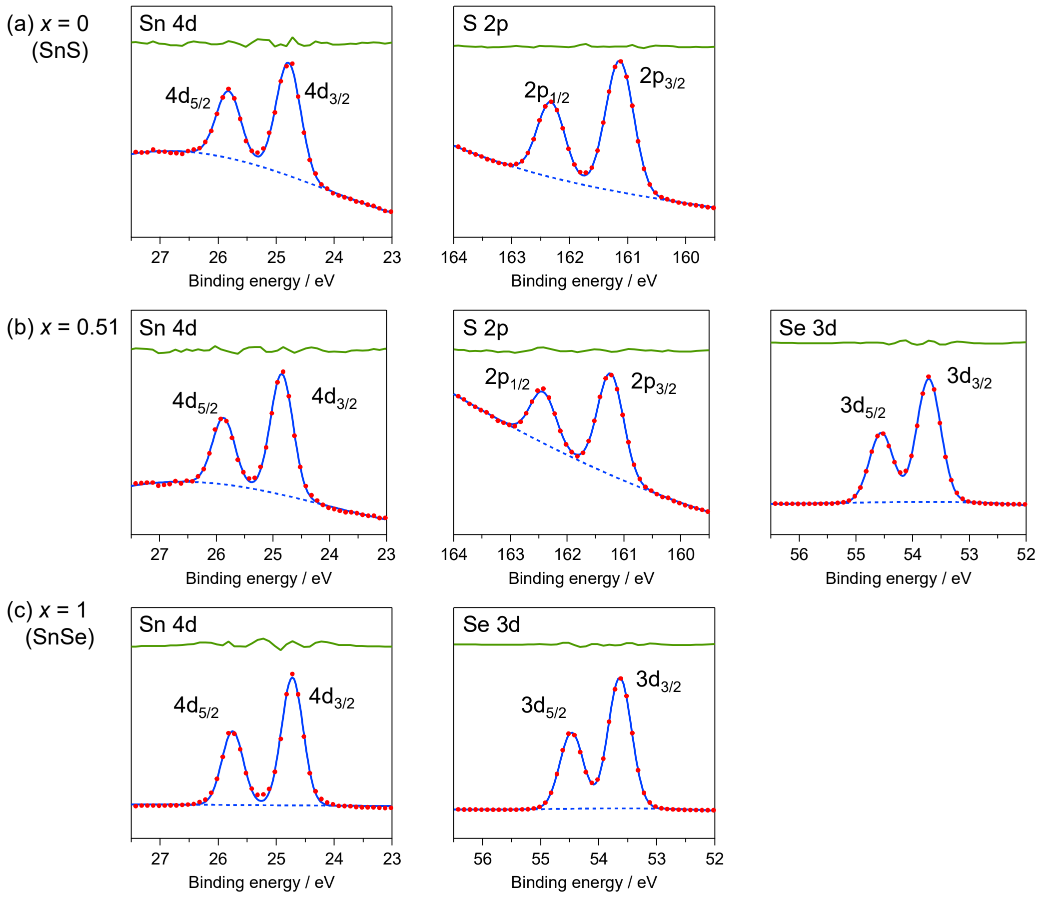

Figure S2. Gaussian peak fitting for Sn 4d, S 2p, and Se 3d core levels for (a) $x = 0$ (SnS), (b) 0.51, and (c) 1(SnSe) in $\mathrm{SnS}_{1-x}\mathrm{Se}_x$. Red dots represent the measurement points. Blue lines and broken lines correspond to the fitted curves and backgrounds, respectively. Green lines indicate the residuals. The wide-range spectra are shown in Figure S3. Details of the fitted peaks were summarized in Table S1.

Table S1. Peak position and Gaussian width of the Gaussian peak fitting performed in Figure S2. Peak area ratio of $d_{5/2}$ to $d_{3/2}$ and of $p_{1/2}$ to $p_{3/2}$ are close to their identical value of 2/3 and 1/2, respectively.

		Peak pos. / eV	Gaussian width / eV	Relative peak area
x=0 (SnS)				
Sn	$4d_{3/2}$	24.79	0.30	1
	$4d_{5/2}$	25.82 (+1.03)	0.30	0.59
S	$2p_{3/2}$	161.14	0.34	1
	$2p_{1/2}$	162.32 (+1.18)	0.34	0.56
x=0.51				
Sn	$4d_{3/2}$	24.84	0.28	1
	$4d_{5/2}$	25.87 (+1.03)	0.28	0.55
S	$2p_{3/2}$	161.24	0.32	1
	$2p_{1/2}$	161.42 (+1.18)	0.32	0.53
Se	$3d_{3/2}$	53.72	0.30	1
	$3d_{5/2}$	54.55 (+0.83)	0.30	0.56
x=1 (SnSe)				
Sn	$4d_{3/2}$	24.72	0.26	1
	$4d_{5/2}$	25.75 (+1.03)	0.26	0.58
Se	$3d_{3/2}$	53.64	0.29	1
	$3d_{5/2}$	54.47 (+0.83)	0.29	0.58

Section 3. XPS spectra of the $SnS_{1-x}Se_x$ single crystals

Figure S3 shows the survey XPS spectra of the $SnS_{1-x}Se_x$ single crystals after cleavage with an excitation source of 180 eV. Assuming that the ratio of Sn to VI-group elements (S/Se) is 1 in each solid solution, the compositions of the solid solutions are determined from the peak areas of Sn 4d, S 2p, and Se 3d, as shown in Table S2. The composition of the surface determined by XPS is in good agreement with the bulk composition determined by EDX.

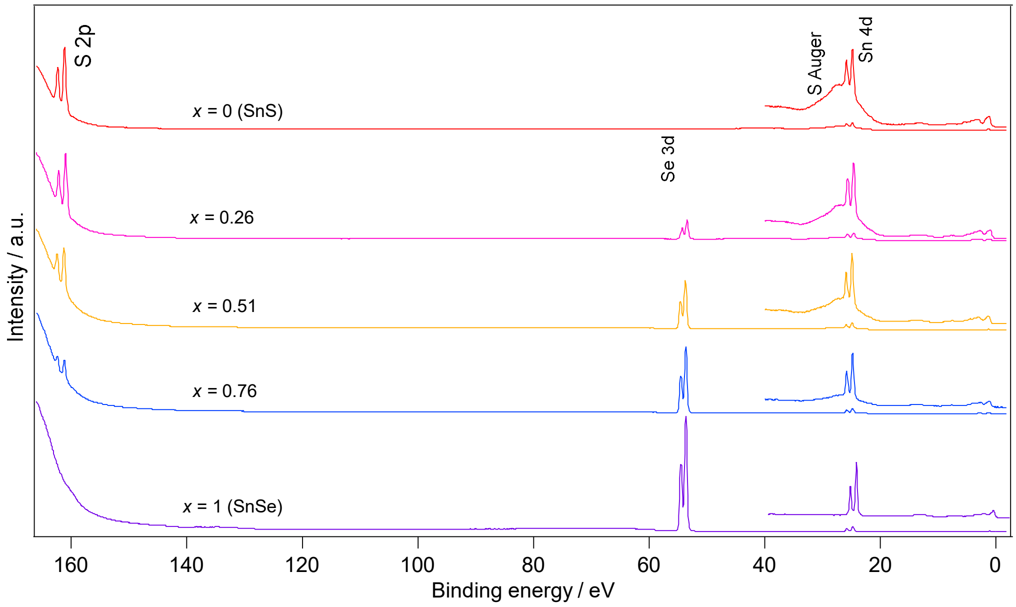

Figure S3. Survey spectra of $SnS_{1-x}Se_x$ single crystal with an excitation source of 180 eV.

Table S2. Relative peak area of XPS spectra for each core level. Surface and bulk compositions were determined by XPS and EDX measurement of single-crystalline $SnS_{1-x}Se_x$ solid solutions, respectively.

Relative peak area			x_{XPS}	x_{EDX}
Sn	S	Se		
1	1	0	0	0 (SnS)
1	0.76	0.20	0.21	0.26
1	0.53	0.44	0.46	0.51
1	0.26	0.71	0.73	0.76
1	0	1	1	1 (SnSe)

Section 4. Dispersion of SnS along k_x direction.

The dispersion perpendicular to the sample surface (i.e., k_x direction in this study) was evaluated by ARPES measurements with different excitation energies (19–27 eV), as shown in Figure S4. Br-doped n-type SnS single crystals [S3] were measured. The measurements were conducted in a BL7U of UVSOR-III at the Institute for Molecular Science. No change in the energies of the observed bands was present even though a slight change in the relative intensity was present, indicating almost no dispersion along the k_x direction in SnS.

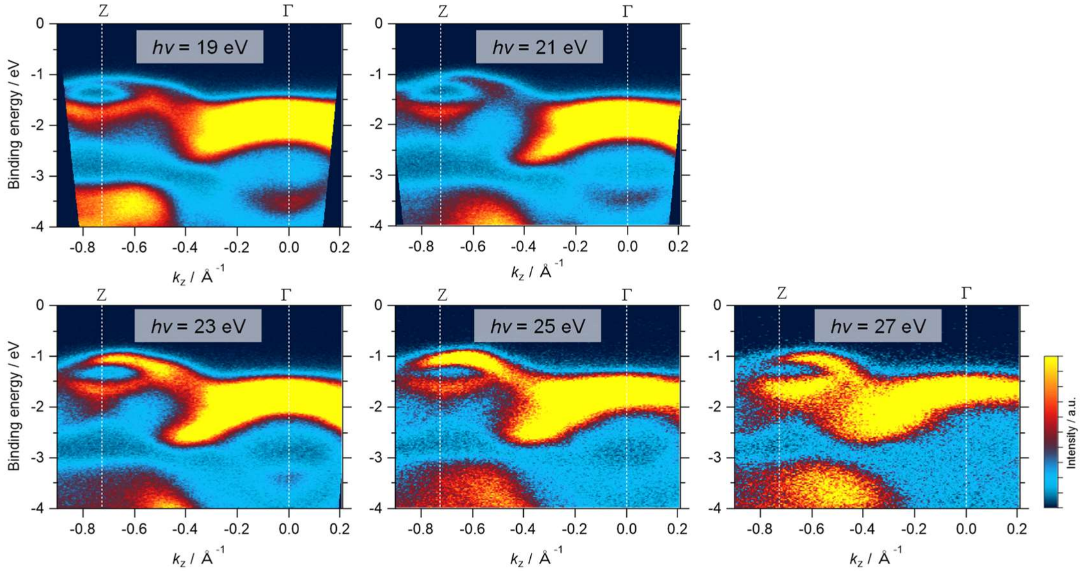

Figure S4. Band dispersion images along Γ-Z direction of SnS single crystal for various excitation energies.

Section 5. Linearly plotted dispersion images of VBM1 along the Γ-Y direction.

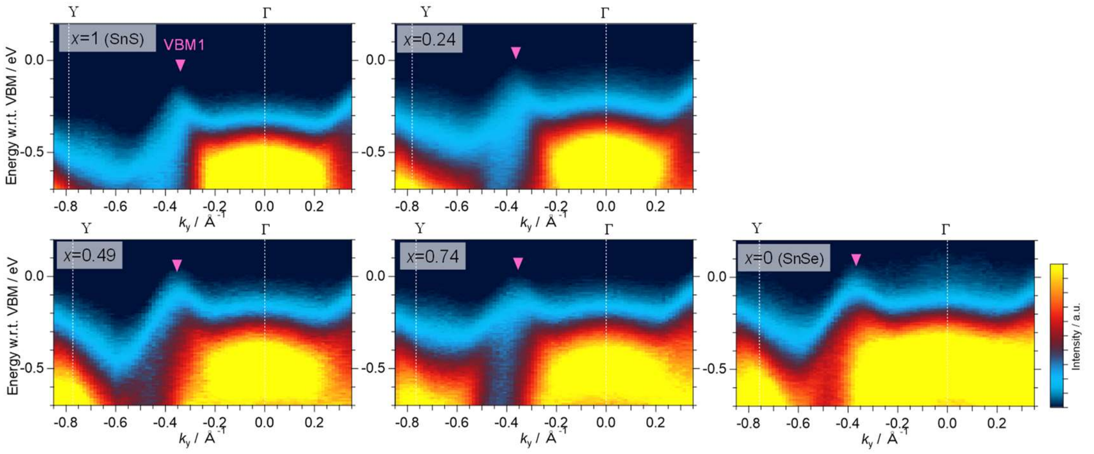

Figure S5. Band dispersion images of VBM1 along k_y direction. The triangles indicate the position of VBM1. Log-scale plotted version is displayed in the main text as Figure 2(c).

References for ESI

[S1] R. Katsube, Y. Nose, Thermodynamic considerations on interfacial reactivity concerning carrier transport characteristics in metal/p-Zn_3P_2 junctions, *J. Mater. Chem. C*, 2017, **5**, 5538–5543

[S2] Y. Nose, T. Takemura, R. Katsube, Jpn. Pat. JP2019072172, 2019.

[S3] S. Kawanishi, I. Suzuki, T. Ohsawa, N. Ohashi, H. Shibata, and T. Omata, Growth of large single crystals of n-type SnS from halogen-added Sn flux, *Crystal Growth & Design*, 2020, **20**, 5931–5939.